

## Article

# Structure Sensitivity of Ammonia Synthesis on Cobalt: Effect of the Cobalt Particle Size on the Activity of Promoted Cobalt Catalysts Supported on Carbon

Magdalena Zybert <sup>1,\*</sup>, Aleksandra Tarka <sup>1</sup>, Wojciech Patkowski <sup>1</sup>, Hubert Ronduda <sup>1</sup>, Bogusław Mierzwa <sup>2</sup>, Leszek Kępiński <sup>3</sup> and Wioletta Raróg-Pilecka <sup>1,\*</sup>

<sup>1</sup> Faculty of Chemistry, Warsaw University of Technology, Noakowskiego 3, 00-664 Warsaw, Poland

<sup>2</sup> Institute of Physical Chemistry, Polish Academy of Sciences, Kasprzaka 44/52, 01-224 Warsaw, Poland

<sup>3</sup> Institute of Low Temperature and Structure Research, Polish Academy of Sciences, Okólna 2, 50-950 Wrocław, Poland

\* Correspondence: magdalena.zybert@pw.edu.pl (M.Z.); wioletta.pilecka@pw.edu.pl (W.R.-P.)

**Abstract:** This work presents a size effect, i.e., catalyst surface activity, as a function of active phase particle size in a cobalt catalyst for ammonia synthesis. A series of cobalt catalysts supported on carbon and doped with barium was prepared, characterized (TEM, XRPD, and H<sub>2</sub> chemisorption), and tested in ammonia synthesis (9.0 MPa, 400 °C, H<sub>2</sub>/N<sub>2</sub> = 3, 8.5 mol% of NH<sub>3</sub>). The active phase particle size was varied from 3 to 45 nm by changing the metal loading in the range of 4.9–67.7 wt%. The dependence of the reaction rate expressed as TOF on the active phase particle size revealed an optimal size of cobalt particles (20–30 nm), ensuring the highest activity of the cobalt catalyst in the ammonia synthesis reaction. This indicated that the ammonia synthesis reaction on cobalt is a structure-sensitive reaction. The observed effect may be attributed to changes in the crystalline structure, i.e., the appearance of the hcp Co phase for the particles with a diameter of 20–30 nm.

**Keywords:** structure sensitivity; size effect; cobalt catalyst; ammonia synthesis; carbon support



**Citation:** Zybert, M.; Tarka, A.; Patkowski, W.; Ronduda, H.; Mierzwa, B.; Kępiński, L.; Raróg-Pilecka, W. Structure Sensitivity of Ammonia Synthesis on Cobalt: Effect of the Cobalt Particle Size on the Activity of Promoted Cobalt Catalysts Supported on Carbon. *Catalysts* **2022**, *12*, 1285. <https://doi.org/10.3390/catal12101285>

Academic Editor: Gilles Berhault

Received: 26 September 2022

Accepted: 19 October 2022

Published: 21 October 2022

**Publisher's Note:** MDPI stays neutral with regard to jurisdictional claims in published maps and institutional affiliations.



**Copyright:** © 2022 by the authors. Licensee MDPI, Basel, Switzerland. This article is an open access article distributed under the terms and conditions of the Creative Commons Attribution (CC BY) license (<https://creativecommons.org/licenses/by/4.0/>).

## 1. Introduction

The structure sensitivity of a reaction [1–4] is a concept established in the 1960s when Boudart noticed that among the reactions carried out in the presence of heterogeneous catalysts, there are those where the rate changes with the size (diameter) of the active phase particles [1]. Van Santen also reported that an increase in the size of metal particles may cause changes in the reaction rate expressed as TOF (turnover frequency), i.e., the activity of a single active site of a catalyst [4]. It was also pointed out that the reaction rate may increase or reach its maximum and then decrease with increasing particle size. However, when considering a size effect, i.e., TOF as a function of metal particle size, it should be underlined that the surface structure may also change with changes in particle size. The popular terrace-ledge-kink (TLK) model assumes the heterogeneity of a surface structure connected with the presence of steps, kinks, adatoms, and vacancies. In the case of very small metal particles or their larger clusters, it is more appropriate to describe the surface structure using the coordination model, where the atoms present on the surface differ from the atoms inside the particle by having an incomplete set of adjacent atoms. Therefore, surface atoms are described by a coordination number, i.e., the number of nearest adjacent atoms (e.g., the C<sub>i</sub> atom has *i* other atoms adjacent to it, while the B<sub>j</sub> active site has *j* closest neighbors). When the particle size of the catalyst's active phase changes, the surface structure also differs because the relative concentration of the surface atoms and active sites changes. Their number increases with the increasing crystallite size. Some studies have shown that the presence of atoms or active sites with specific coordination can be attributed to the high activity of the catalyst [5,6]. Different particle sizes may also favor the formation of various crystallographic structures of the active phase [7].

The catalytic reaction of hydrogen and nitrogen in the presence of iron, leading to the formation of ammonia, is a prime example of a reaction highly dependent on the structure of the active phase [5,8–16]. Ertl et al. showed that dissociative nitrogen adsorption, i.e., the rate-determining step of the  $\text{NH}_3$  synthesis reaction, strongly depends on the iron surface structure [8,9]. The activity of the investigated iron surfaces in relation to dissociative nitrogen adsorption changes in the order  $\text{Fe} (111) > \text{Fe} (100) > \text{Fe} (110)$  [8]. This sequence is consistent with the results obtained by Samoraj et al. [5,10,13], where it was observed that the  $\text{Fe} (111)$  and  $\text{Fe} (211)$  surfaces are much more active in the synthesis of ammonia than the  $\text{Fe} (100)$ ,  $\text{Fe} (210)$ , and  $\text{Fe} (110)$ . It was found that the differences in the activity of these structures result directly from the arrangement of Fe atoms and, more specifically, from their coordination. The  $\text{Fe} (111)$  is the best Fe single crystal surface for  $\text{NH}_3$  synthesis [16]. The high activity of the  $\text{Fe} (111)$  surface is related to the presence of C7 atoms, i.e., Fe atoms with seven nearest neighbors [5]. Assuming that the surface structure of iron particles may change with their size, Dumesic et al. investigated the properties of supported iron catalysts ( $\text{Fe}/\text{MgO}$ ) with iron particles of different sizes ( $d = 1.5, 4, 10, 30 \text{ nm}$ ) [11,12]. The research confirmed that the activity in ammonia synthesis (TOF) increases with the increasing size of iron particles. This effect was explained by a lower number of C7 atoms on the surface of smaller particles [11]. They also noticed that the pretreatment of the iron catalyst of small Fe particles in a nitrogen atmosphere may cause a reconstruction of the iron crystallites surface, and the concentration of C7 atoms may be increased [12]. Theoretical studies of bcc Fe surface using DFT calculation and micro-kinetics analysis [14] revealed that  $\text{Fe} (211)$ ,  $(310)$ , and  $(221)$  surfaces, which consist of active C7 and/or B5 sites, dominate the overall reactivity when iron particles are larger than 6 nm. Further decreasing the particle size to 2.3–6 nm, the corresponding TOF is two or three times lower due to the absence of the highly active  $\text{Fe} (221)$  surface. However, the reactivity is substantially reduced for particles smaller than 2 nm because no active C7 and/or B5 sites are exposed.

Numerous studies also indicate that the ammonia synthesis reaction on the ruthenium catalyst is structure-sensitive [6,17–22]. Dahl et al. [17–19] showed that the  $\text{N}_2$  dissociation on the  $\text{Ru} (0001)$  surface is dominated by steps (at least 9 orders of magnitude higher than on the terraces), which is a result of a combination of electronic and geometrical effects coexisting in the ruthenium catalyst. Jacobsen et al. stated [6] that B5 sites, i.e., a system of five atoms with a specific configuration, are responsible for the high activity of ruthenium. Van Hardeveld and van Montfoort also observed the presence of B5 sites on the platinum, palladium, and nickel surfaces [20], indicating that these sites are responsible for strong nitrogen adsorption. Both the studies of van Hardeveld [20] and Jacobsen [6] showed that the number of B5 sites depends on the size of metal crystallites. In the case of particles smaller than 1 nm, B5 sites' contribution to the metal surface is small. Their number increases with increasing particle size reaching the maximum for particles in the range of 1.8–2.5 nm and gradually decreasing for larger particles [6]. Studies of ruthenium catalysts in the ammonia synthesis reaction revealed that the reaction rate is a function of the Ru crystallite size. Liang showed [21] that TOF increased with an increase in the average Ru crystallite size in the range of 1.7–10.3 nm for the promoted catalyst supported on carbon ( $\text{Ru-K}/\text{C}$ ). In the work [22], Raróg-Pilecka et al. also reported that with increasing ruthenium content on the carbon support in the range of 1–32 wt%, the average size of Ru crystallites increased monotonically from 1 nm to 4 nm and along with it, the activity (TOF) increased. It was also noted that extrapolation of the TOF value for crystallites smaller than the examined one suggests that very fine ruthenium crystallites (i.e., smaller than 0.7–0.8 nm) may be completely inactive in the ammonia synthesis reaction (a critical size). Li et al. [23] reported that sub-nanometric Ru catalysts not only exhibit performance different from that of NPs, but also follow a different route for  $\text{N}_2$  activation.

Ammonia synthesis is a structure-sensitive reaction when conducted in the presence of a cobalt catalyst. Rambeau noted that cobalt's activity in this reaction strongly depends on its allotropic form [24]. The hexagonal close-packed (hcp) phase has twice the activity (expressed as TOF) of the face-centered cubic (fcc) phase. Density functional theory (DFT)

calculations showed that the activity of the hcp Co (101 $\bar{2}$ ) and hcp Co (112 $\bar{1}$ ) surfaces in the N<sub>2</sub> dissociation process significantly exceeds the activity of the other surfaces, which is reflected in the high activity of the hcp cobalt phase in the ammonia synthesis reaction [25]. However, the effect of cobalt particle size on the catalytic properties of cobalt catalysts in ammonia synthesis has not been documented so far.

This study aimed to investigate the effect of cobalt particle size on the activity of the cobalt catalyst in the ammonia synthesis reaction. A series of barium-promoted cobalt catalysts supported on graphitized carbon was prepared. As reported in the previous studies of our group [26,27] and other researchers [28,29], this type of catalyst is a promising alternative system for the synthesis of ammonia, exhibiting higher activities at synthesis temperatures than the commercial, multipromoted iron catalyst as well as a lower ammonia inhibition. Co is normally quite inert toward N<sub>2</sub> dissociation, and as a result it shows low activity in ammonia synthesis reactions. Hence, the addition of a barium promoter is required to boost its performance. The promoting effect of barium results not only from its electronic and/or structural influence [30,31], but, according to the latest research [32], is related to the reduction of the spin polarization of the neighboring Co atoms defining the active site for N<sub>2</sub> dissociation. The promoted cobalt systems deposited on a carrier represent a good object for studying the particle-size dependence of activity. In the present studies, the active phase particle size was varied by changing the metal loading in the range of 4.9–67.7 wt%. The characterization of cobalt particle size was carried out using the chemisorption method (H<sub>2</sub>-TPD). The sorption experiments were supplemented with XRPD and TEM measurements. An in-depth discussion of the Co particle size–NH<sub>3</sub> catalyst activity relationship was provided, and the optimal Co particle size ensuring the most favorable catalytic properties of the cobalt systems was determined.

## 2. Results

### 2.1. Characterization of a Carbon Support

The material used as support was a modified carbon of a well-developed texture. The total surface area and total pore volume were 1611 m<sup>2</sup> g<sup>−1</sup> and 1.02 cm<sup>3</sup> g<sup>−1</sup>, respectively. A significant contribution of micropores was observed, which accounted for 85% of the total surface area and 80% of the total porosity. This characteristic is essential for preparing highly loaded Ba-Co/C catalysts of high metal dispersion [26]. The structural analysis showed that the support exhibited features characteristic of turbostratic carbon [33–36], having structural ordering between the amorphous carbon phase and crystalline graphite phase. In the diffraction pattern depicted in Figure 1a, the broad reflections derived from the (002) and (004) planes and asymmetric (10) signal characteristic of turbostratic carbon were visible. Moreover, a sharp reflex at 2θ = 26.2°, assigned to the presence of a small amount of graphite in the support, was observed. The size of turbostratic stacks in the (002) direction was approximately 1 nm, and the average size of graphite stacks was approximately 6 nm (both values were estimated based on Scherrer's equation). The parallel graphene layers visible in the TEM image (Figure 1b) and the carbon-derived rings in the selected area electron diffraction (SAED) pattern (Figure 1c) confirmed the partial graphitization of the carbon support.

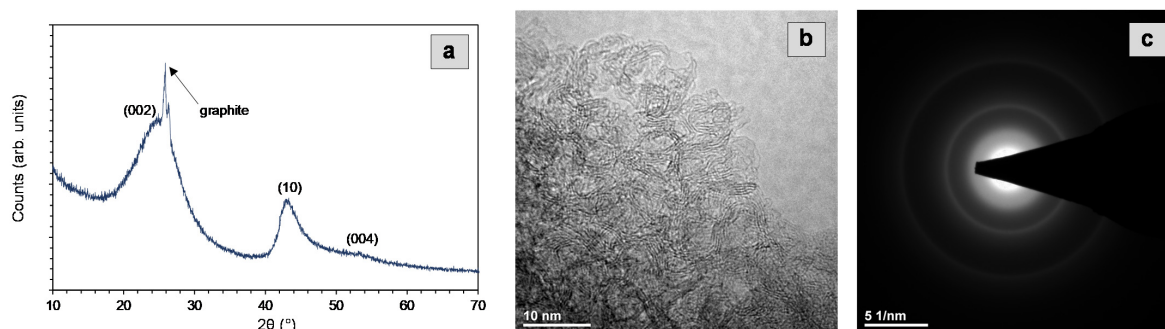


**Figure 1.** The structure of the carbon support: (a) XRPD pattern, (b) HRTEM image, (c) SAED pattern.

## 2.2. Characterization of the Active Phase (Cobalt) Particles

Structural characterization (TEM and XRPD) studies were carried out for the Ba-Co/C catalysts previously tested in  $\text{NH}_3$  synthesis reaction (i.e., the spent catalysts after exposure to air—ex situ measurements). The diffraction profiles for the catalysts are depicted in Figure 2. The reflections at  $2\theta = 44.2^\circ$ ,  $51.5^\circ$ ,  $75.9^\circ$ , and  $92.2^\circ$  corresponding to the fcc Co phase were identified for all the tested samples. As expected, the contribution of cobalt to the diffraction profiles strongly depended on the metal loading. The intensity of the reflections assigned to the fcc Co phase increased with increasing Co content, which suggested an increase in the crystallinity of this phase. The most intensive reflections corresponded to the catalysts with the highest metal content (Ba-Co43.1/C and Ba-Co67.7/C). For these systems, the fcc Co signals were asymmetric, which can be assigned to stacking faults or the presence of mixed fcc Co and hcp Co phases. Low-intensity signals at  $2\theta = 41.7^\circ$  and  $47.6^\circ$  can be attributed to the hcp Co phase. Moreover, the reflections at  $2\theta = 43^\circ$  and  $79^\circ$  assigned to carbon were observed for all the catalysts. No reflections indicating the presence of barium compounds were recorded, suggesting their good dispersion or amorphous form. The average size of cobalt crystallites estimated based on fcc Co reflections ( $d_{\text{Co-fcc}}$ ) is presented in Table 1. The smallest Co crystallites of 14 nm were observed for the sample with the lowest metal content (Ba-Co4.9/C) and the largest crystallites of 25 nm for the catalyst with the highest Co content (Ba-Co67.7/C). For other systems, cobalt crystallites were of similar size (approximately 20 nm).

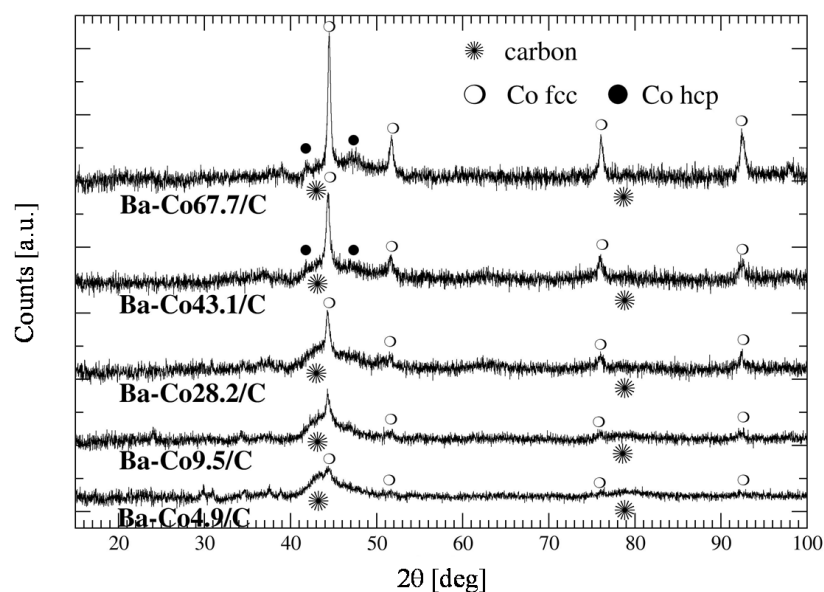


**Figure 2.** XRPD patterns of the Ba-Co/C catalysts (the spent catalysts after exposure to air—ex situ measurements).

**Table 1.** Average cobalt crystallite and cobalt particle size in the Ba-Co/C catalysts based on XRPD and TEM measurements (the spent catalysts after exposure to air—ex situ measurements).

Catalyst	$d_{\text{Co-fcc}}^1$ (nm)	$d_{\text{core-shell}}^2$ (nm)	$d_{\text{core}}^3$ (nm)
Ba-Co4.9/C	14	—	—
Ba-Co9.5/C	21	20	15
Ba-Co28.2/C	19	26	19
Ba-Co43.1/C	18	22	16
Ba-Co67.7/C	25	41	31

<sup>1</sup> the average cobalt crystallite size determined based on the Co fcc reflections from the XRPD measurements; <sup>2</sup> the average size of the “core-shell” particles observed by TEM; <sup>3</sup> the average size of the metallic core of the particles observed by TEM.

TEM investigations (Figure 3) revealed that differences in the cobalt particle size were obtained depending on the active phase content. Changes in the size and number of Co particles on the support surface were clearly visible for the catalysts with cobalt content: 4.9 wt% (Figure 3a), 48.1 wt% (Figure 3b) and 67.7 wt% (Figure 3c). The preparation procedure enabled to obtain catalysts with sufficient dispersion (i.e., with a high Co particle density per support surface unit) even when the active phase content was relatively high (e.g., Ba-Co43.1/C, Figure 3b). Moreover, it was observed that in the studied catalysts, the cobalt particles were either partially (on the surface) or fully oxidized. The particles with a diameter smaller than 10 nm were almost entirely oxidized (Figure 4a), whereas the larger particles formed a “core-shell” type structure (Figure 4b) with a core of metallic cobalt surrounded by an oxide layer. Cobalt oxidation is due to exposure of the catalysts to air after their removal from the ammonia synthesis reactor (ex situ TEM measurements). This caused some difficulties in terms of an adequate cobalt particle size estimation during TEM experiments, especially for the catalysts, where small particles (<10 nm) dominated (Ba-Co4.9/C). The contribution of these particles increased with the decrease of the total Co content in the sample. Therefore, the error in the average particle size determination increased for the catalysts of low Co content.

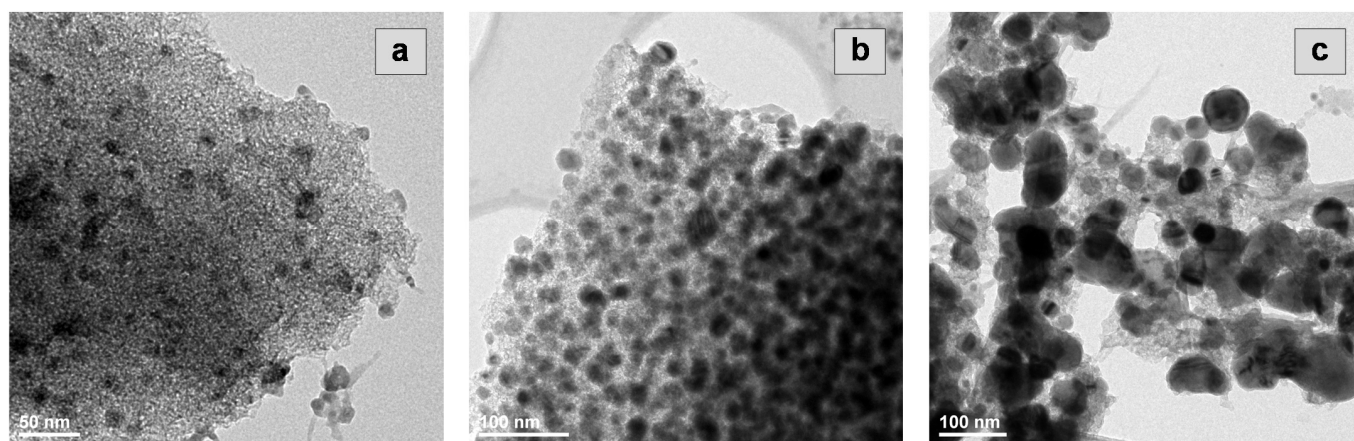


**Figure 3.** TEM images of the selected catalysts of (a) low (Ba-Co4.9/C), (b) medium (Ba-Co43.1/C), and (c) high (Ba-Co67.7/C) cobalt content (the spent catalysts after exposure to air—ex situ measurements).

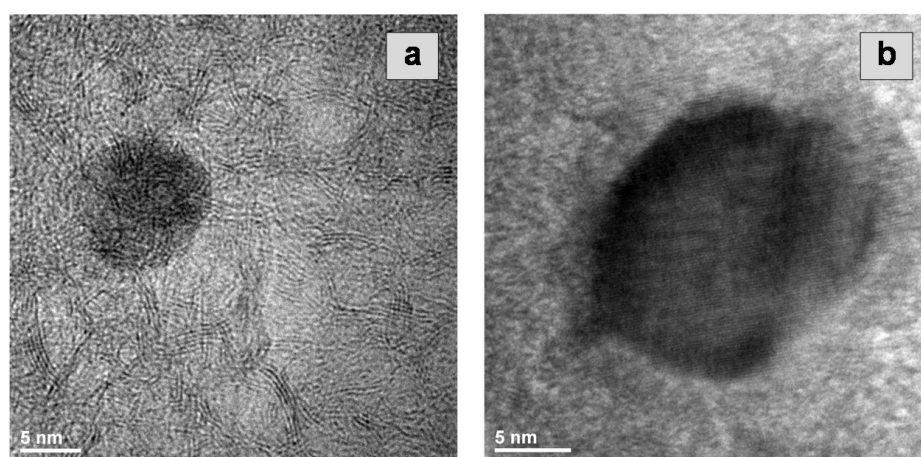


**Figure 4.** HRTEM images of a single Co particle: (a) entirely oxidized—Ba-Co4.9/C catalyst, (b) surrounded by an oxide layer—“core-shell” structure of Ba-Co28.2/C catalyst (the spent catalysts after exposure to air—ex situ measurements).

The average size of core-shell particles ( $d_{\text{core-shell}}$ ) and the average size of a metallic core ( $d_{\text{core}}$ ) estimated based on TEM results are presented in Table 1. The average size of

the metallic core was the largest for the catalyst with the highest Co content (Ba-Co67.7/C) and exceeded 30 nm. For other systems,  $d_{\text{core}}$  values were similar. The average size of the metallic core was in good agreement with the average cobalt crystallite size ( $d_{\text{Co-fcc}}$ ) determined by XRPD (Table 1).

Figure 5 depicts the profiles of hydrogen desorption from the surface of the selected catalysts of low (Ba-Co4.9/C), medium (Ba-Co43.1/C), and high (Ba-Co67.7/C) cobalt content. Two signals of similar characteristics but different intensities were observed on the profiles of all the studied catalysts. The low-temperature signal with a maximum at ca. 100 °C corresponded to hydrogen desorption from weakly binding adsorption sites. The high-temperature signal with a maximum of 410–500 °C was assigned to the presence of strongly binding hydrogen adsorption sites. However, one can see from Figure 5 that, depending on the cobalt content in the catalyst, adsorption sites of different natures dominated on the surface of the active phase. In the catalyst of low cobalt content (Ba-Co (4.9)/C), the similar intensity of both signals indicated the presence of a comparable number of adsorption sites weakly and strongly binding hydrogen with a slight predominance of weak adsorption sites. In the case of the Ba-Co (43.1)/C catalyst, adsorption sites of low hydrogen binding strength were more pronounced. Strong hydrogen binding sites clearly dominated on the surface of the catalyst with the highest active phase content (Ba-Co (67.7)/C).

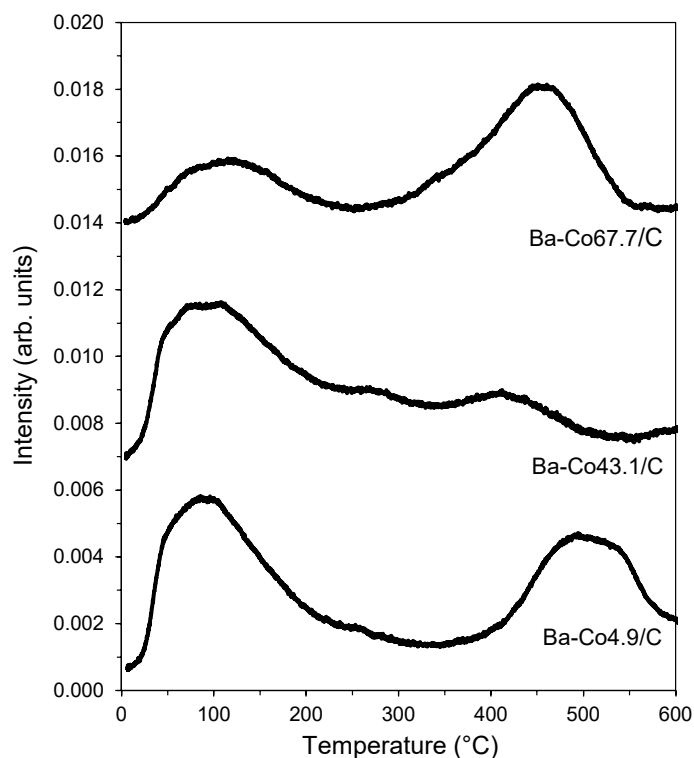


**Figure 5.** H<sub>2</sub>-TPD profiles of the selected catalysts of low (Ba-Co4.9/C), medium (Ba-Co43.1/C), and high (Ba-Co67.7/C) cobalt content.

The results of the quantitative analysis of the obtained desorption profiles are summarized in Table 2. As indicated by the blank experiments, hydrogen was not adsorbed either on the carbon support or the barium promoter. Hence, the adsorbate (H<sub>2</sub>) uptake was ascribed entirely to the presence of cobalt. The data revealed that the content of the active phase strongly influenced its adsorption on the support surface and, thus, the metal particle size. It is observed that the more cobalt the catalyst contained, the lower its dispersion (FE) and the greater particle size ( $d_{\text{Co}}$ ). However, using a carbon support of well-developed texture and the proper preparation procedure, a wide range of Co particle sizes was obtained, from 3 nm for the Ba-Co4.9/C catalyst to 45 nm for the Ba-Co67.7/C catalyst. It should also be noted that a high degree of the active phase dispersion on carbon

was achieved even with a high metal loading. Comparing the cobalt crystallite size and cobalt particle size (Table 1) with the  $d_{\text{Co}}$  values determined by the chemisorption method (Table 2), it is noticeable that the  $d_{\text{Co}}$  values were smaller than those estimated by the XRPD or TEM methods. The difference was especially pronounced for the samples with low cobalt content (4.9 and 9.5 wt% Co). However, it should be remembered that XRPD and TEM measurements were performed ex situ. Due to the tendency of the reduced catalysts to oxidize when contacted with air, the size of Co crystallites and particles estimated by these methods might be overestimated.

**Table 2.** Chemisorptive characteristics of the Ba-Co/C catalysts.

Catalyst	H <sub>2</sub> Uptake ( $\mu\text{mol g}_{\text{Co}}^{-1}$ )	FE (%) <sup>1</sup>	$d_{\text{Co}}$ (nm) <sup>2</sup>
Ba-Co4.9/C	2740	32.5	3
Ba-Co9.5/C	1530	18.0	7
Ba-Co28.2/C	850	9.5	13
Ba-Co43.1/C	540	6.3	20
Ba-Co52.9/C	330	3.9	33
Ba-Co59.4/C	270	3.2	39
Ba-Co67.7/C	240	2.8	45

<sup>1</sup> FE (fraction exposed)—the active phase (cobalt) dispersion defined as the ratio of surface cobalt atoms to total cobalt atoms in the catalyst sample; <sup>2</sup> the average Co particle size in the catalyst sample.

### 2.3. Catalyst Activity

Figure 6 illustrates the effect of the cobalt particle size ( $d_{\text{Co}}$ ) calculated from hydrogen chemisorption on the activity of the Ba-Co/C catalysts expressed as an average reaction rate ( $r$ ) and surface reaction rate (TOF). It is clearly visible that the activity of the cobalt catalysts in the NH<sub>3</sub> synthesis reaction depended on the particle size of the active phase. The average reaction rate ( $r$ ) increased with increasing cobalt particle size ( $d_{\text{Co}}$ ), reached a maximum value for particles of about 20 nm in diameter, and decreased for the bigger particles. In the case of the surface reaction rate (TOF), the highest value was observed for cobalt particles in the range of 20–30 nm. An increase or decrease in the Co particle size beyond this range decreased the TOF value. Moreover, extrapolation of the results towards small particle diameters may suggest that extra fine particles, i.e., smaller than 0.5 nm, might be totally inactive (a critical size).

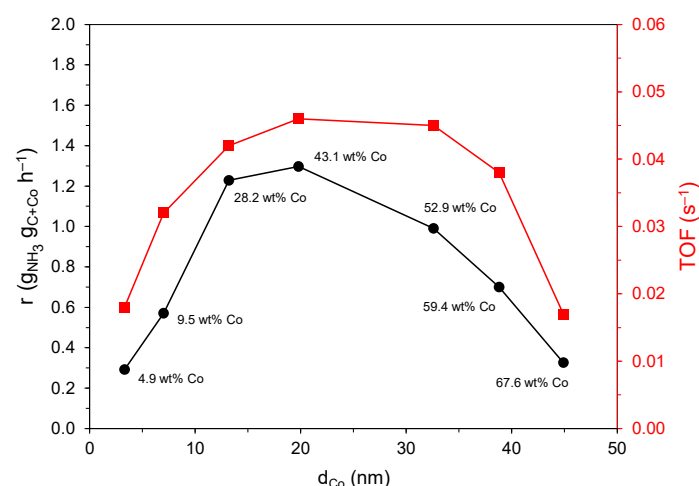


**Figure 6.** Dependence of activity of the Ba-Co/C catalysts on the cobalt particle size ( $d_{\text{Co}}$ ). Activity expressed as an average NH<sub>3</sub> synthesis reaction rate ( $r$ ) and surface reaction rate (TOF); measurement conditions:  $T = 400^\circ\text{C}$ ,  $p = 9.0\text{ MPa}$ ,  $\text{H}_2 + \text{N}_2 + \text{NH}_3$  flow rate  $70\text{ dm}^3\text{ h}^{-1}$ ,  $\text{H}_2/\text{N}_2 = 3$ ,  $x_{\text{NH}_3} = 8.5\text{ mol}\%$ ; TOF determined based on average reaction rate ( $r$ ) values and the hydrogen chemisorption data. (Values marked by the points indicate the cobalt content in the catalysts corresponding to the crystallites of a given size. Ba content in all the catalysts was  $1\text{ mmol g}_{\text{C}}^{-1}$ ).

On this basis, it can be concluded that ammonia synthesis conducted on the cobalt catalyst is a structure-sensitive reaction. The obtained dependence (Figure 6) revealed the existence of an optimal size of cobalt particles (20–30 nm), ensuring the highest activity of the catalyst. This observation is of great importance for the implementation of the studied catalysts. It has been found that using a support with a well-developed texture and the proper preparation procedure, the Ba-Co/C cobalt catalysts with high Co content and optimal active phase particle size can be obtained. This, in turn, transfers into a high activity in the ammonia synthesis reaction.

The comparison of the catalytic performance (expressed as the reaction rate) of the selected, most active among the studied catalysts and other Ba-Co/C catalysts previously described in the literature [26,27] is presented in Table 3. Under the same measurement conditions, the studied catalysts showed higher activity than other Ba-Co/C catalysts of similar composition. Moreover, the reaction rate for the studied catalysts is almost four times higher than for the commercial iron catalyst (KM I).

**Table 3.** The comparison of the reaction rate of ammonia synthesis over the different cobalt catalysts and commercialized iron catalyst (KM I). Reaction conditions:  $T = 400\text{ }^{\circ}\text{C}$ ,  $p = 9.0\text{ MPa}$ ,  $\text{H}_2 + \text{N}_2 + \text{NH}_3$  flow rate  $70\text{ dm}^3\text{ h}^{-1}$ ,  $\text{H}_2/\text{N}_2 = 3$ ,  $x_{\text{NH}_3} = 8.5\text{ mol}\%$ .

Catalyst	$r_{\text{NH}_3}$ ( $\text{g}_{\text{NH}_3}\text{ g}_{(\text{C}+\text{Co})}^{-1}\text{ h}^{-1}$ )	Reference
Ba-Co28.2/C	1.23	This work
Ba-Co43.1/C	1.30	This work
Ba-Co22.8N/B	0.86	[26]
Ba-Co25.4 <sub>N(R/P+C)</sub> /B	1.05	[26]
Ba-Co <sub>R+P+C</sub> /C	0.65	[27]
KM I	0.33	[26]

### 3. Discussion

In trying to explain the correlation between the reactivity of the cobalt surface in ammonia synthesis and the particle size of the active phase, three issues should be considered: (1) the interaction between cobalt particles and carbon support, (2) the structure sensitivity of the ammonia synthesis reaction on cobalt, and (3) the presence of a promoter in the Ba-Co/C catalyst.

(1) Electron-withdrawing functional groups, primarily those containing oxygen, covering the surface of carbon, can interact with cobalt particles causing the decrease of catalytic activity of their surface in the ammonia synthesis reaction. This is due to the fact that electron-poor surfaces are less active in dissociative adsorption of nitrogen, i.e., the rate-determining step of ammonia synthesis. This phenomenon was previously reported by Aika et al. [37–39] for Ru/C systems. The negative impact of oxygen complexes on the surface activity of ruthenium was also observed by Raróg-Pilecka et al. [40] in the reaction of ammonia decomposition over Ru/C catalysts. Presumably, a similar effect may occur for the studied cobalt catalyst supported on carbon. In this respect, it should be expected that the adverse interaction of the oxygen-containing groups would diminish with increasing cobalt particle size and thus result in the increased surface activity of the catalysts expressed as TOF. However, such a relationship was not observed in the discussed systems (Figure 6). A systematic increase in catalyst activity (TOF) was observed for small and medium-size particles ( $d_{\text{Co}} \leq 20\text{ nm}$ ). In the case of the catalysts with  $d_{\text{Co}}$  sizes in the range of 20–30 nm, the highest activity was observed, followed by its gradual decrease with a further increase in cobalt particle size. Moreover, the activated carbon used for preparing Ba-Co/C catalysts was subjected to high-temperature processing ( $1900\text{ }^{\circ}\text{C}$ ), which led to a deep purification of carbon, including the removal of surface functional groups. The additional gasification in a mixture of water vapor-argon performed after high-temperature annealing led to the formation of new oxygen groups on the carbon surface. However, as shown in [41], the number of these groups is insignificant. Therefore, the carbon-cobalt interaction cannot explain the TOF vs  $d_{\text{Co}}$  dependence (Figure 6).

(2) The second possibility of interpreting the correlation between the reactivity of the cobalt surface in ammonia synthesis (TOF) and the Co particle size ( $d_{Co}$ ) is the structure sensitivity of the ammonia synthesis reaction. As noted in the Section 1, this phenomenon is related to the size of the metal particles on the surface of which the reaction takes place. The results of the conducted research revealed (Figure 6) that there is an optimal size of cobalt particles (20–30 nm), for which the highest activity was obtained in the ammonia synthesis reaction. However, it has been reported in the literature [42] that the maximum concentration of highly coordinated sites (i.e., highly active sites) was obtained for cobalt crystallites with a size of 2–6 nm. The observed discrepancy may result from the assumptions that the metal particles were formed by well-defined crystallites, which shape, morphology and structure did not change with the increase of their diameter. However, the possibility that in the Co/C systems, these structural properties of cobalt crystallites may change as the particles increase cannot be ruled out. According to Kitakami et al. [7], there is a close relationship between the cobalt particle size and the crystal phase. It was shown that particles of diameter  $\leq 20$  nm crystallize in the fcc Co phase, whereas there is a mixture of the fcc Co and hcp Co phases in crystallites with a diameter of ca. 30 nm. For particles with a diameter  $\geq 40$  nm, the hcp Co phase dominates with only a small amount of the fcc Co phase. According to Rambeau et al. [24], the activity of cobalt in  $NH_3$  synthesis strongly depends on the metal structure and is twice higher for the hcp Co phase than for the fcc Co phase. In this respect, the shift of the optimal Co particle size towards higher values (about 20 nm) seems understandable for the studied catalysts. The hcp Co phase appeared for the particles with a diameter of 20–30 nm, and there was still a significant contribution of the surface cobalt atoms (a sufficient dispersion). However, XRPD studies (Figure 2) revealed that the fcc Co phase dominated in the Ba-Co/C catalysts. The hcp Co phase started to be noticeable in the diffraction patterns of the catalysts with Co particle size ( $d_{Co}$ , Table 2) of ca. 20 nm and bigger (the Ba-Co43.1/C and Ba-Co67.7/C, Figure 2). Nevertheless, these studies were performed ex situ. Therefore, the possibility that, under the reaction conditions, a greater amount of the hcp Co phase may be present in the cobalt particles of optimal size cannot be ruled out. Advanced in situ experiments are necessary to clarify this issue thoroughly.

(3) The character of TOF vs.  $d_{Co}$  dependence (Figure 6) may presumably in some extent be related to the presence of a promoter in the Ba-Co/C catalyst. The possibility of some characteristic, preferential placement of the barium promoter on cobalt particles of a specific size cannot be ruled out. Assuming that the barium promoter located on the flat surfaces of Co particles causes an increase in the catalytic activity of the adjacent cobalt atoms, a systematic increase of the TOF value with increasing Co particle size should be expected, as one can see in Figure 6. The maximum can be quite broad because it results from the way of particle growth (small particles can be round, but larger particles can be rather flat). A decrease in the activity is observed only for bigger Co particles ( $\geq 40$  nm), in which the ratio of surface cobalt atoms to all cobalt atoms is very small (low dispersion—Table 2). Thus, the addition of a barium promoter to the Co/C system may result either in a change of activity of active sites already existing on the Co surface or the formation of new sites with particularly advantageous catalytic properties in the ammonia synthesis reaction, but only for the particles of medium size (20–30 nm). The observed, opposite to the expected, phenomenon, i.e., a decrease in activity for cobalt particles of larger size (i.e., particles  $\geq 40$  nm with a greater fraction of the hcp phase) is an intriguing issue and the explanation is not obvious. In order to confirm the presented hypothesis about the influence of the presence of barium, further and more thorough investigation is required, which may shed light on this issue.

## 4. Materials and Methods

### 4.1. Catalyst Preparation

The activated carbon GF40 (Norit, Glasgow, UK) was used as support for preparing the Ba-Co/C catalysts. Briefly, starting carbon (extrusions of 2 mm in diameter) was subjected

to two-step modification: (1) heating at 1900 °C for 2 h in argon flow, (2) gasification in water vapor/argon flow at 865 °C for 5 h up to 32 wt% of mass loss. Then, the carbon material was washed with distilled water and dried at 120 °C for 18 h in air.

The Ba-Co/C catalysts of different cobalt content in the range of 4.9 to 67.7 wt% were synthesized by the wet impregnation method. An appropriate amount of cobalt nitrate hexahydrate ( $\text{Co}(\text{NO}_3)_2 \cdot 6\text{H}_2\text{O}$ , Acros Organics, Thermo Fischer Scientific, Kandel, Germany) was dissolved in ethanol, and carbon support was added to this solution. After impregnation for 24 h, the solvent was evaporated under reduced pressure. Then, calcination in argon flow was carried out at 200 °C for 18 h. For the catalysts containing more than 10 wt% Co, the impregnation procedure and subsequent calcination in argon were repeated until the required Co content was obtained. After the last impregnation, materials were calcined at 200 °C for 18 h in air. To obtain the Ba-promoted catalysts, the calcined samples were impregnated with an aqueous solution of barium nitrate ( $\text{Ba}(\text{NO}_3)_2$ , Chempur, Karlsruhe, Germany,  $130 \text{ g dm}^{-3}$ ) at 90 °C for 16 h to obtain a constant and optimal Ba content in all the catalysts equal to  $1 \text{ mmol g}_C^{-1}$ . Subsequently, the solid materials were separated from the hot solution and dried at 90 °C for 18 h in air. The obtained materials were crushed and sieved to get a 0.2–0.63 mm fraction. The catalyst samples were denoted as Ba-Co(x)/C, where x is the Co content (wt%) in an unpromoted material (estimated based on the mass balance before and after impregnation and final calcination).

#### 4.2. Catalyst Characterization

The textural parameters of carbon support were determined by nitrogen physisorption using an ASAP2020 instrument (Micromeritics Instrument Co., Norcross, GA, USA). Before the measurements, the sample was degassed in vacuum in two stages: at 90 °C for 1 h and then at 300 °C for 4 h. The total surface area and total pore volume were estimated using the Brunauer-Emmett-Teller (BET) and Barrett-Joyner-Halenda (BJH) adsorption isotherm models, respectively.

The phase composition of carbon support and the selected catalysts (the spent catalysts after exposure to air; ex situ measurements) was determined using X-ray powder diffraction (XRPD). Data were collected with a Siemens D5000 diffractometer (München, Germany) in a Bragg-Brentano configuration using a Cu-sealed tube operating at 40 kV and 40 mA with a Ni filter. Each sample was measured in the scattering angle range of 5° to 100° with a 0.02° step and a counting speed of  $1.0 \text{ s step}^{-1}$ . The average size of cobalt crystallites and graphite/graphite-like packages were determined from Scherrer's equation using the integral width of reflections fitted to the analytical Pearson VII functions.

TEM images were recorded with a Philips CM20 Super Twin microscope (Amsterdam, the Netherlands), which provides a 0.25 nm resolution at 200 kV. The samples for TEM studies were prepared by grinding the materials in a mortar and then dispersing them in methanol. A droplet of the suspension was placed on a microscope grid covered with a perforated carbon film.

The  $\text{H}_2$  chemisorption measurements were carried out in a fully automated AutoChem 2920 instrument (Micromeritics Instrument Co., Norcross, GA, USA) equipped with a TCD detector and supplied with high purity (6N) gases. The catalyst sample of 0.2 g was reduced in  $\text{H}_2$  flow ( $40 \text{ cm}^3 \text{ min}^{-1}$ ) at 520 °C at a ramping rate of  $10 \text{ °C min}^{-1}$  for 20 h. Next, the gas flow was switched to argon ( $40 \text{ cm}^3 \text{ min}^{-1}$ ) for purging the sample at 600 °C for 45 min and then cooling the sample to 150 °C. Then, the  $\text{H}_2$  adsorption was carried out at 150 °C for 15 min, during cooling the sample to 0 °C and then at 0 °C for 15 min. After rinsing the sample with argon ( $40 \text{ cm}^3 \text{ min}^{-1}$ ) at 0 °C for 1 h to remove weakly adsorbed hydrogen, the catalyst was heated in argon flow ( $40 \text{ cm}^3 \text{ min}^{-1}$ ) to 600 °C with a  $10 \text{ °C min}^{-1}$  temperature ramp and the concentration of  $\text{H}_2$  in the outlet gas was monitored ( $\text{H}_2$ -TPD). Consequently, the amount of hydrogen evolved to the gas phase was determined by integrating the  $\text{H}_2$  desorption profile. The  $\text{H}_2$ -TPD data were used for calculating the cobalt dispersion expressed as FE (fraction exposed, i.e., the number of surface Co atoms related to the total number of Co atoms) and the average size of cobalt particles

( $d_{Co}$ ). The H/Co = 1 stoichiometry [43] and the formula proposed by Borodziński and Bonarowska [44] were used to determine FE and  $d_{Co}$ .

#### 4.3. Activity Measurements

The kinetic measurements of  $NH_3$  synthesis were carried out in a differential reactor supplied with a high purity (>99.9999%) stoichiometric  $H_2-N_2-NH_3$  mixture of controlled ammonia concentration ( $x_1$ ). A detailed description of the apparatus and methodology can be found elsewhere [45,46]. Briefly, under steady-state conditions of temperature (400 °C), gas flow rate (70 dm<sup>3</sup> h<sup>-1</sup>), pressure (9.0 MPa), and ammonia concentration in the inlet gas (8.5 mol% of  $NH_3$ ), small increments ( $x_2$ ) in the concentration of ammonia formed on the catalyst due to the reaction were measured interferometrically. Consequently, the  $NH_3$  synthesis rate was determined. Typically, small catalyst samples (0.5 g, fraction of 0.2–0.63 mm) were used in the studies. Before the experiments, reduction (activation) of the samples was performed in  $H_2/N_2 = 3$  flow (40 dm<sup>3</sup> h<sup>-1</sup>) at 0.1 MPa following the temperature program: 400 °C (20 h) → 470 °C (24 h) → 520 °C (24 h).

## 5. Conclusions

A series of barium-promoted cobalt catalysts supported on graphitized carbon was prepared, characterized, and tested in the ammonia synthesis reaction. The active phase particle size was varied from 3 to 45 nm by changing the metal loading in the range of 4.9–67.7 wt%. The characterization of cobalt particles revealed a correlation between the reactivity of the cobalt surface in ammonia synthesis and the particle size of the active phase—the phenomenon of structure sensitivity of the reaction. The dependence of the reaction rate expressed as TOF on the particle size of the active phase indicated that there is an optimal size of cobalt particles (20–30 nm), ensuring the highest activity of the cobalt catalyst in the ammonia synthesis reaction. Increasing or decreasing the particle size caused a decrease in activity, even leading to the expected total loss of catalyst activity for fine Co particles (smaller than 0.5 nm). The size effect may be most likely attributed to changes in Co crystalline structure. For the particles with a diameter of 20–30 nm, the hcp Co phase (more active than the fcc Co phase) appeared, and there was still a significant contribution of the surface cobalt atoms (a sufficient dispersion) conducive to higher activity.

**Author Contributions:** Conceptualization, A.T., M.Z. and W.R.-P.; methodology, A.T., M.Z. and W.R.-P.; investigation, M.Z., A.T., H.R., W.P., B.M., L.K. and W.R.-P.; writing—original draft preparation, M.Z.; writing—review and editing, M.Z., H.R. and W.R.-P.; visualization, H.R.; supervision, M.Z. and W.R.-P.; funding acquisition, A.T. All authors have read and agreed to the published version of the manuscript.

**Funding:** This research was financially supported by the National Science Centre, Poland (Research project No. 2016/23/N/ST5/00685).

**Data Availability Statement:** All data is available within the paper.

**Conflicts of Interest:** The authors declare no conflict of interest.

## References

1. Boudart, M. Catalysis by Supported Metals. *Adv. Catal.* **1969**, *20*, 153–166. [[CrossRef](#)]
2. Somorjai, G.A.; Carrazza, J. Structure sensitivity of catalytic reactions. *J. Ind. Eng. Chem. Fundam.* **1986**, *25*, 63–69. [[CrossRef](#)]
3. Somorjai, G.A. The structure sensitivity and insensitivity of catalytic reactions in light of the adsorbate induced dynamic restructuring of surfaces. *Catal. Lett.* **1990**, *7*, 169–182. [[CrossRef](#)]
4. Van Santen, R.A. Complementary structure sensitive and insensitive catalytic relationships. *Acc. Chem. Res.* **2009**, *42*, 57–66. [[CrossRef](#)] [[PubMed](#)]
5. Strongin, D.R.; Carrazza, J.; Bare, S.R.; Somorjai, G.A. The importance of C7 sites and surface roughness in the ammonia synthesis reaction over iron. *J. Catal.* **1987**, *103*, 213–215. [[CrossRef](#)]
6. Jacobsen, C.J.H.; Dahl, S.; Hansen, P.L.; Törnqvist, E.; Jensen, L.; Topsøe, H.; Prip, D.V.; Møenshaug, P.B.; Chorkendorff, I. Structure sensitivity of supported ruthenium catalysts for ammonia synthesis. *J. Mol. Catal. A Chem.* **2000**, *163*, 19–26. [[CrossRef](#)]

7. Kitakami, O.; Sato, H.; Shimada, Y.; Sato, F.; Tanaka, M. Size effect on the crystal phase of cobalt fine particles. *Phys. Rev. B* **1997**, *56*, 13849–13854. [[CrossRef](#)]
8. Bozso, F.; Ertl, G.; Grunze, M.; Weiss, M. Interaction of nitrogen with iron surfaces: I. Fe(100) and Fe(111). *J. Catal.* **1977**, *49*, 18–41. [[CrossRef](#)]
9. Bozso, F.; Ertl, G.; Weiss, M. Interaction of nitrogen with iron surfaces: II. Fe(110). *J. Catal.* **1977**, *50*, 519–529. [[CrossRef](#)]
10. Spencer, N.D.; Schoonmaker, R.C.; Somorjai, G.A. Iron single crystals as ammonia synthesis catalysts: Effect of surface structure on catalyst activity. *J. Catal.* **1982**, *74*, 129–135. [[CrossRef](#)]
11. Dumesic, J.A.; Topsøe, H.; Khammouma, S.; Boudart, M. Surface, catalytic and magnetic properties of small iron particles: II. Structure sensitivity of ammonia synthesis. *J. Catal.* **1975**, *37*, 503–512. [[CrossRef](#)]
12. Dumesic, J.A.; Topsøe, H.; Boudart, M. Surface, catalytic and magnetic properties of small iron particles: III. Nitrogen induced surface reconstruction. *J. Catal.* **1975**, *37*, 513–522. [[CrossRef](#)]
13. Somorjai, G.A.; Materer, N. Surface structures in ammonia synthesis. *Top. Catal.* **1994**, *1*, 215–231. [[CrossRef](#)]
14. Zhang, B.-Y.; Su, H.-Y.; Liu, J.-X.; Li, W.-X. Interplay Between Site Activity and Density of BCC Iron for Ammonia Synthesis Based on First-Principles Theory. *ChemCatChem* **2019**, *11*, 1928–1934. [[CrossRef](#)]
15. Parker, I.B.; Waugh, K.C.; Bowker, M. On the structure sensitivity of ammonia synthesis on promoted and unpromoted iron. *J. Catal.* **1988**, *114*, 457–459. [[CrossRef](#)]
16. Qian, J.; An, Q.; Fortunelli, A.; Nielsen, R.J.; Goddard, W.A., III. Reaction Mechanism and Kinetics for Ammonia Synthesis on the Fe(111) Surface. *J. Am. Chem. Soc.* **2018**, *140*, 6288–6297. [[CrossRef](#)]
17. Dahl, S.; Logadottir, A.; Egeberg, R.C.; Larsen, J.H.; Chorkendorff, I.; Törnqvist, E.; Nørskov, J.K. Role of Steps in N<sub>2</sub> Activation on Ru(0001). *Phys. Rev. Lett.* **1999**, *83*, 1814–1817. [[CrossRef](#)]
18. Dahl, S.; Törnqvist, E.; Chorkendorff, I. Dissociative adsorption of N<sub>2</sub> on Ru(0001): A surface reaction totally dominated by steps. *J. Catal.* **2000**, *192*, 381–390. [[CrossRef](#)]
19. Dahl, S.; Sehested, J.; Jacobsen, C.J.H.; Törnqvist, E.; Chorkendorff, I. Surface science based microkinetic analysis of ammonia synthesis over ruthenium catalysts. *J. Catal.* **2000**, *192*, 391–399. [[CrossRef](#)]
20. Van Hardeveld, R.; Van Montfoort, A. The influence of crystallite size on the adsorption of molecular nitrogen on nickel, palladium and platinum: An infrared and electron-microscopic study. *Surf. Sci.* **1966**, *4*, 396–430. [[CrossRef](#)]
21. Liang, C.; Wei, Z.; Xin, Q.; Li, C. Ammonia synthesis over Ru/C catalysts with different carbon supports promoted by barium and potassium compounds. *Appl. Catal. A Gen.* **2001**, *208*, 193–201. [[CrossRef](#)]
22. Raróg-Pilecka, W.; Miśkiewicz, E.; Szmigiel, D.; Kowalczyk, Z. Structure sensitivity of ammonia synthesis over promoted ruthenium catalysts supported on graphitized carbon. *J. Catal.* **2005**, *231*, 11–19. [[CrossRef](#)]
23. Li, L.; Jiang, Y.-F.; Zhang, T.; Cai, H.; Zhou, Y.; Lin, B.; Lin, X.; Zheng, Y.; Zheng, L.; Wang, X.; et al. Size sensitivity of supported Ru catalysts for ammonia synthesis: From nanoparticles to subnanometric clusters and atomic clusters. *Chem* **2022**, *8*, 749–768. [[CrossRef](#)]
24. Rambeau, G.; Jorti, A.; Amariglio, H. Catalytic activity of a cobalt powder in NH<sub>3</sub> synthesis in relation with the allotropic transformation of the metal. *J. Catal.* **1985**, *94*, 155–165. [[CrossRef](#)]
25. Zhang, B.Y.; Chen, P.-P.; Liu, J.-X.; Su, H.-Y.; Li, W.-X. Influence of Cobalt Crystal Structures on Activation of Nitrogen Molecule: A First-Principles Study. *J. Phys. Chem. C* **2019**, *123*, 10956–10966. [[CrossRef](#)]
26. Raróg-Pilecka, W.; Miśkiewicz, E.; Kepiński, L.; Kaszukur, Z.; Kielar, K.; Kowalczyk, Z. Ammonia synthesis over barium-promoted cobalt catalysts supported on graphitized carbon. *J. Catal.* **2007**, *249*, 24–33. [[CrossRef](#)]
27. Raróg-Pilecka, W.; Miśkiewicz, E.; Matyszek, M.; Kaszukur, Z.; Kepiński, L.; Kowalczyk, Z. Carbon-supported cobalt catalyst for ammonia synthesis: Effect of preparation procedure. *J. Catal.* **2006**, *237*, 207–210. [[CrossRef](#)]
28. Hagen, S.; Barfod, R.; Fehrmann, R.; Jacobsen, C.J.H.; Teunissen, H.T.; Chorkendorff, I. Ammonia synthesis with barium-promoted iron–cobalt alloys supported on carbon. *J. Catal.* **2003**, *214*, 327–335. [[CrossRef](#)]
29. Hagen, S.; Barfod, R.; Fehrmann, R.; Jacobsen, C.J.H.; Teunissen, H.T.; Stahl, K.; Chorkendorff, I. New efficient catalyst for ammonia synthesis: Barium-promoted cobalt on carbon. *Chem. Commun.* **2002**, *11*, 1206–1207. [[CrossRef](#)]
30. Raróg-Pilecka, W.; Karolewska, M.; Truskiewicz, E.; Iwanek, E.; Mierzwa, B. Cobalt catalyst doped with cerium and barium obtained by Co-precipitation method for ammonia synthesis process. *Catal. Lett.* **2011**, *141*, 678–684. [[CrossRef](#)]
31. Tarka, A.; Patkowski, W.; Zybert, M.; Ronduda, H.; Wieciński, P.; Adamski, P.; Sarnecki, A.; Moszyński, D.; Raróg-Pilecka, W. Synergistic Interaction of Cerium and Barium—New Insight into the Promotion Effect in Cobalt Systems for Ammonia Synthesis. *Catalysts* **2020**, *10*, 658. [[CrossRef](#)]
32. Cao, A.; Bukas, V.J.; Shadravan, V.; Wang, Z.; Li, H.; Kibsgaard, J.; Chorkendorff, I.; Nørskov, J.K. A spin promotion effect in catalytic ammonia synthesis. *Nat. Commun.* **2022**, *13*, 2382. [[CrossRef](#)]
33. Li, Z.Q.; Lu, C.J.; Xia, Z.P.; Zhou, Y.; Luo, Z. X-ray diffraction patterns of graphite and turbostratic carbon. *Carbon* **2007**, *45*, 1686–1695. [[CrossRef](#)]
34. Kowalczyk, Z.; Sentek, J.; Jodzis, S.; Diduszko, R.; Presz, A.; Terzyk, A.; Kucharski, Z.; Suwalski, J. Thermally modified active carbon as a support for catalysts for NH<sub>3</sub> synthesis. *Carbon* **1996**, *34*, 403–409. [[CrossRef](#)]
35. Toth, P. Nanostructure quantification of turbostratic carbon by HRTEM image analysis: State of the art, biases, sensitivity and best practices. *Carbon* **2021**, *178*, 688–707. [[CrossRef](#)]

36. Ruz, P.; Banerjee, S.; Pandey, M.; Sudarsan, V.; Sastry, P.U.; Kshirsagar, R.J. Structural evolution of turbostratic carbon: Implications in H<sub>2</sub> storage. *Solid State Sci.* **2016**, *62*, 105–111. [[CrossRef](#)]
37. Zhong, Z.; Aika, K. The Effect of Hydrogen Treatment of Active Carbon on Ru Catalysts for Ammonia Synthesis. *J. Catal.* **1998**, *173*, 535–539. [[CrossRef](#)]
38. Zhong, Z.; Aika, K. Effect of ruthenium precursor on hydrogen-treated active carbon supported ruthenium catalysts for ammonia synthesis. *Inorg. Chem. Acta* **1998**, *280*, 183–188. [[CrossRef](#)]
39. Aika, K.; Hori, H.; Ozaki, A. Activation of nitrogen by alkali metal promoted transition metal I. Ammonia synthesis over ruthenium promoted by alkali metal. *J. Catal.* **1972**, *27*, 424–431. [[CrossRef](#)]
40. Raróg-Pilecka, W.; Szmigiel, D.; Komornicki, A.; Zieliński, J.; Kowalczyk, Z. Catalytic properties of small ruthenium particles deposited on carbon: Ammonia decomposition studies. *Carbon* **2003**, *41*, 589–591. [[CrossRef](#)]
41. Bonarowska, M.; Raróg-Pilecka, W.; Karpiński, Z. The use of active carbon pretreated at 2173 K as a support for palladium catalysts for hydrodechlorination reactions. *Catal. Today* **2011**, *169*, 223–231. [[CrossRef](#)]
42. Van Hardeveld, R.; Hartog, F. The statistics of surface atoms and surface sites on metal crystals. *Surf. Sci.* **1969**, *15*, 189–230. [[CrossRef](#)]
43. Reuel, R.C.; Bartholomew, C.H. The stoichiometries of H<sub>2</sub> and CO adsorptions on cobalt: Effects of support and preparation. *J. Catal.* **1984**, *85*, 63–77. [[CrossRef](#)]
44. Borodziński, A.; Bonarowska, M. Relation between Crystallite Size and Dispersion on Supported Metal Catalysts. *Langmuir* **1997**, *13*, 5613–5620. [[CrossRef](#)]
45. Kowalczyk, Z. Effect of potassium on the high pressure kinetics of ammonia synthesis over fused iron catalyst. *Catal. Lett.* **1996**, *37*, 173–179. [[CrossRef](#)]
46. Ronduda, H.; Zybert, M.; Patkowski, W.; Tarka, A.; Ostrowski, A.; Raróg-Pilecka, W. Kinetic studies of ammonia synthesis over a barium-promoted cobalt catalyst supported on magnesium–lanthanum mixed oxide. *J. Taiwan Inst. Chem. Eng.* **2020**, *114*, 241–248. [[CrossRef](#)]